

QUANTUM SPECTRUM ON THE NAKED REISSNER-NORDSTRÖM BACKGROUND

V.D. Gladush¹, D.A. Kulikov²

Theoretical Physics Department, Dniepropetrovsk National University
72 Gagarin av., Dniepropetrovsk 49010, Ukraine,
¹vgladush@gmail.com, ²kulikov_d_a@yahoo.com,

ABSTRACT. The eigen frequencies of a massless scalar field in the space-time of the Reissner-Nordström singularity are studied by using the WKB approximation and by numerical integration of the wave equation. Both these approaches indicate the existence of long living states for the singularity charge-to-mass ratios being close enough to the extremal value $Q/M = 1$.

Key words: naked singularity, scalar field, bound state, Reissner–Nordström metric.

1. Introduction

The Reissner-Nordström (RN) solution describes electrovacuum in general relativity. If the electric charge exceeds the central mass, $Q > M$, this solution corresponds to a naked singularity. Quantum excitations on the naked RN geometry have recently attracted considerable attention; in particular, quasinormal modes (QNMs) of the massless scalar field were calculated [Chirenti]. On the other hand, it was shown [Gladush] that metastable bound states (MBSs) with the longer live-times may also exist in the same case.

The purpose of this work is to compare the frequencies (energies) of the different scalar field excitations that emerge on the naked RN background among themselves and with the frequency extracted from numerical evaluation of probe signal propagation.

2. Wave equation and effective potential

Consider the massless Klein-Gordon equation $\square\psi = 0$ in the external RN geometry

$$ds^2 = F dt^2 - F^{-1} dr^2 - r^2 d\sigma^2, \\ F = 1 - \frac{2M}{r} + \frac{Q^2}{r^2}, \quad d\sigma^2 = d\theta^2 + \sin^2\theta d\varphi^2. \quad (1)$$

Introducing the tortoise coordinate x by $dx = F^{-1}dr$ and seeking for the solution with angular variables separated, $\psi = \exp(-i\omega t)Y_{lm}(\theta, \varphi)\phi(x)/r$, one obtains

$$\frac{d^2\phi}{dx^2} + [\omega^2 - \mathcal{V}(r(x))]\phi = 0, \\ \mathcal{V}(r(x)) = \left[\frac{l(l+1)}{r^2(x)} + \frac{2M}{r^3(x)} - \frac{2Q^2}{r^4(x)} \right] \cdot F(r(x)). \quad (2)$$

To establish possible types of the solutions, one inspects the shape of the effective potential $\mathcal{V}(r)$. It is shown [Chirenti] that there are essentially two different cases: (i) for $Q/M < (Q/M)_{cr}$, $\mathcal{V}(r)$ has one maximum, (ii) for $Q/M > (Q/M)_{cr}$, $\mathcal{V}(r)$ has 3 extrema, one smaller "outer" maximum, one "inner" maximum and minimum in the potential valley between them. Here the critical value $(Q/M)_{cr} = 1.048, 1.056, 1.059, \dots$ for $l=0,1,2,\dots$. It tends to $(Q/M)_{cr} = \sqrt{9/8} \approx 1.061$ when $l \rightarrow \infty$ [Chirenti]. In Fig. 1 $\mathcal{V}(r)$ is plotted to illustrate those two cases. Since the dependence $r(x)$ is monotonous the plot of \mathcal{V} versus x has similar shape.

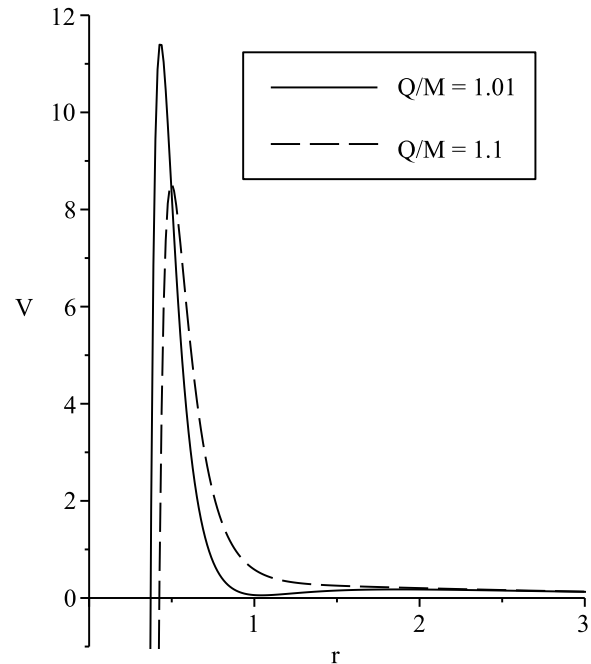


Figure 1: Effective potential $\mathcal{V}(r)$ for $l = 1$ and $M = 1$, $Q = 1.01$ (solid line) and $M = 1$, $Q = 1.1$ (dashed line).

3. Spectrum via WKB approximation

The above suggests that apart from the scattering states there may be two different types of the quasis-

tationary states, namely, QNMs near the top of one of the effective potential peaks and MBSs in the potential valley between peaks.

The QNM spectrum of the problem in the WKB approximation reads as [Chirenti]

$$\omega = \sqrt{\mathcal{V}(r_{max})} - i(n+1/2)F(r_{max})\sqrt{-\frac{\mathcal{V}''(r_{max})}{2\mathcal{V}(r_{max})}} \quad (3)$$

with r_{max} being the position of the "outer" maximum, n being the excitation number and the prime denoting the derivative with respect to r .

The WKB approximation for the eigen frequencies of the MBSs has been developed in [Gladush] by applying the conventional approach [Landau] to the wave equation rewritten in terms of the areal coordinate r

$$y'' + \frac{1}{F^2}(\omega^2 - V(r))y = 0 \quad (4)$$

where $y = \sqrt{F}\phi(r)$ and $V(r) = \mathcal{V}(r) - (2M/r^3 - 2Q^2/r^4)F + (Q^2 - M^2)/r^4$. The new effective potential $V(r)$ goes very closely to $\mathcal{V}(r)$ except for a small region near the origin. Also $V(r)$ has a potential valley behind a low peak provided that $1 < Q/M < \sqrt{(8 + 9l(l+1))/(8 + 8l(l+1))}$.

Defining quasiclassical momenta $k(r)$ and $\kappa(r)$ for the classically allowed and forbidden regions respectively by

$$k(r) = \frac{1}{F}\sqrt{\omega^2 - V(r)}, \quad \kappa(r) = \frac{1}{F}\sqrt{V(r) - \omega^2}, \quad (5)$$

one can write down the Bohr-Sommerfeld formula

$$\int_{r_1}^{r_2} \frac{1}{F}\sqrt{\omega_R^2 - \mathcal{V}(r)}dr = \pi(n + 1/2) \quad (6)$$

that determines the real part ω_R of the frequency ω of the MBS. Here $r_{1,2}$ are the turning points at the ends of the $V(r)$ potential valley.

For the imaginary part of ω , the Gamow-type formula has been derived [Gladush]

$$\omega_I = \left[4\omega_R \int_{r_1}^{r_2} \frac{dr}{F^2 k(r)} \right]^{-1} e^{-2 \int_{r_2}^{r_3} \kappa(r) dx}, \quad (7)$$

which is valid if the forbidden region (r_2, r_3) (potential barrier represented by the peak of $V(r)$) is nearly impenetrable. It means that the calculated value of ω_I has to obey the condition $|\omega_I| \ll \omega_R$.

For the sake of comparison, another approximation can be made. Since the main contribution to ω_R comes from the region in vicinity of the minimum r_{min} of the potential, one can expand $\mathcal{V}(r)$ in powers of $(r - r_{min})$. On substituting this into wave equation (2) and retaining only the quadratic term, the problem reduces to the harmonic oscillator one with the spectrum

$$\omega_R^2 = \mathcal{V}(r_{min}) + (n + 1/2)F(r_{min})\sqrt{2\mathcal{V}''(r_{min})}. \quad (8)$$

The exponentially small decay width ω_I vanishes in this approximation.

Equation (8) is to be compared with the QNM spectrum (3). One makes sure that the MBS frequencies are indeed concentrated near the bottom of the potential valley whereas the QNMs frequencies near the potential peak.

4. Probe signal propagation

Since the spectrum of the system contains the states of different types and with different frequencies, it is tempting to explore what is the frequency that dominates in the propagation of an "arbitrary" probe signal.

To this end, the numerical method [Gundlach] will be employed that is based on treating the Klein-Gordon equation in terms of the light-cone coordinates $u = t - x$ and $v = t + x$. For the field $\psi = Y_{lm}(\theta, \varphi)\Phi(u, v)/r$, one gets

$$\left(4\frac{\partial^2}{\partial u \partial v} + \mathcal{V}(u, v) \right) \Phi(u, v) = 0. \quad (9)$$

This is simply discretized on a (u, v) grid as

$$\begin{aligned} \Phi(N) &= \Phi(W) + \Phi(E) - \Phi(S) - \\ &- \frac{h^2}{8}\mathcal{V}(S)(\Phi(W) + \Phi(E)) + \mathcal{O}(h^4) \end{aligned} \quad (10)$$

where the points N, S, E and W form a rectangle with relative positions indicated by the points of the compass (see Fig. 2), and h is the integration step, so that

$$\Delta u = u_N - u_E = h, \quad \Delta v = v_N - v_W = h. \quad (11)$$

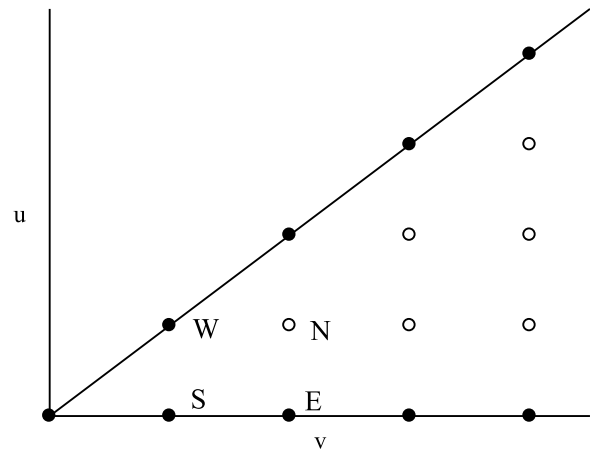


Figure 2: Numerical grid used for integration.

The boundary conditions are chosen as follows

$$\begin{aligned} \Phi(r = 0, t) &= \Phi(u, v = u + 2x(r = 0)) = 0, \\ \Phi(u = 0, v) &= e^{-\frac{(v-v_c)^2}{2\sigma^2}}. \end{aligned} \quad (12)$$

This amounts to the Dirichlet condition in the origin and the data on the $u = 0$ line modelling an "arbitrary" initial signal to be propagated.

Starting from these null data depicted by filled circles in Fig. 2, integration proceeds to the "north" and the field in the points depicted by empty circles is calculated according to algorithm (10).

5. Numerical results

Calculations were made for the case of $Q/M < (Q/M)_{cr}$ because for $Q/M > (Q/M)_{cr}$ it is argued [Chirenti] that there are no low-damped QNMs at least in the $l \gg 1$ limit and the MBSs are absent too [Gladush].

The QNM spectrum was computed according to formula (3) whereas the MBS spectrum was evaluated by means of formulae (6) and (7). It should be noticed that since the depth and the width of the potential valley are finite, the number of the MBSs is limited.

In Table 2 the first QNM frequencies calculated using the values $Q = 1.01$, $M = 1$ are presented.

Table 1: QNM frequencies on the naked RN background with $Q = 1.01$, $M = 1$.

| | |
|---------|------------------------|
| $l = 0$ | |
| $n = 0$ | $0.224344 - i0.092955$ |
| $l = 1$ | |
| $n = 0$ | $0.420128 - i0.088186$ |
| $l = 2$ | |
| $n = 0$ | $0.656772 - i0.087090$ |

For comparison, the frequencies of all the existing MBSs with $l = 1, 2$ (there are no $l = 0$ states) calculated with the same parameters are listed in Table 2.

Table 2: Frequencies of the MBSs on the naked RN background with $Q = 1.01$, $M = 1$.

| | |
|---------|------------------------------------|
| $l = 1$ | |
| $n = 0$ | $0.294636 - i0.263 \times 10^{-3}$ |
| $l = 2$ | |
| $n = 0$ | $0.423194 - i0.164 \times 10^{-5}$ |
| $n = 1$ | $0.537046 - i0.227 \times 10^{-3}$ |

The striking difference between Tables 1 and 2 is that the MBSs have much smaller decay widths and thus are much more long living than the QNMs. This is because the MBSs are concentrated near the bottom of the potential valley and have to penetrate the potential barrier in order to decay.

Using the same parameters, the propagation of the probe signal (12) with $v_c = 1$ and $\sigma = 1$ was computed via scheme (10). In Figs. 3 and 4 the time evolution of the field $\Phi_{l=0}(x, t)$ and $\Phi_{l=1}(x, t)$ at given $x = 10$ is shown. The plotted data were further approximated by the least-squares method to the single mode $\Phi_{app}(t) = Ae^{-\alpha t} \sin(\Omega t + \beta)$ in order to extract the dominant frequency. The results are $\Omega - i\alpha = 0.2015 - i0.552 \times 10^{-2}$

for $l = 0$ and $\Omega - i\alpha = 0.3013 - i0.223 \times 10^{-3}$ for $l = 1$. The last value is remarkably close to the MBS frequency with $l = 1$ and $n = 0$ in Table 2.

Thus the results of both the numerical integration and the WKB approximation indicate that the scalar field on the naked RN background possesses long living excitations. These are associated with the states lying near the bottom of the effective potential valley.

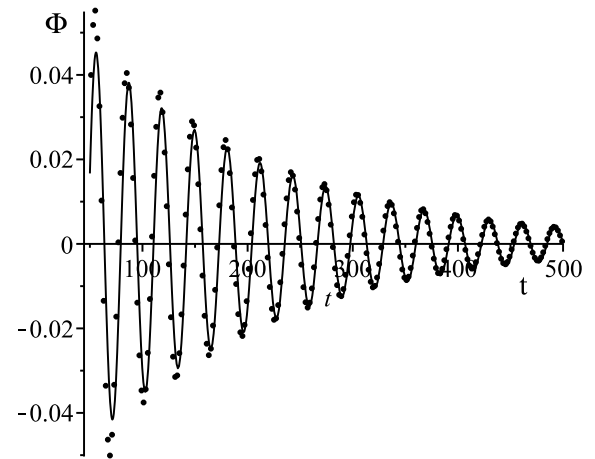


Figure 3: $\Phi(x = 10, t)$ vs. t for $Q = 1.01$, $M = 1$ and $l = 0$. The circles depict the result of integration, the curve is the least-squares single-mode approximation.

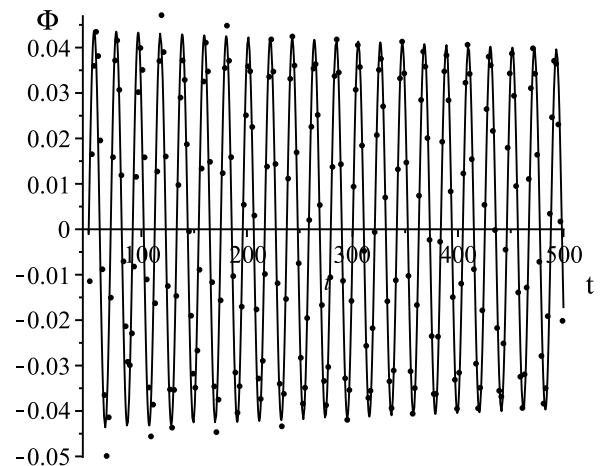


Figure 4: The same as Fig. 3 for $l = 1$.

References

- Chirenti C., Saa A., Skákala J.: 2012, *Phys. Rev. D* **86**, 124008.
 Gladush V.D., Kulikov D.A.: 2013, *Int. J. Mod. Phys. D* **22**, 1350033.
 Landau L.D., Lifshitz E.M. *Quantum Mechanics: Non-relativistic Theory*. Oxford, 1965.
 Gundlach C., Price R.H., Pullin J.: 1994, *Phys. Rev. D* **49**, 883.